

PAPER

Rechargeable Active Implantable Medical Devices (AIMDs)

Deepali Newaskar¹(✉),
B. P. Patil²

¹RMD Sinhgad Technical
Institute Campus, Warje,
Pune, India

²Army Institute of Technology,
Dighi, Pune, India

[deepali.newaskar.rmdssoe@
sinhgad.edu](mailto:deepali.newaskar.rmdssoe@sinhgad.edu)

ABSTRACT

Active Implantable Medical Devices (AIMDs) act as lifesaving devices. They provide electrical signals to tissues as well as perform data-logging operations. To perform these operations, they need power. The battery is the only source for such devices, as they are placed invasively inside the human body. Once the battery drains out, the patient wearing the device has to undergo medical surgery for the second time, where there are many chances of infections, and it could be life-threatening too. If the AIMDs, e.g., pacemakers are designed using rechargeable batteries, then the devices can be recharged regularly, which can increase the life of the device as well as reduce its size. Wireless charging of AIMDs such as ICDs or pacemakers is proposed in this paper using magnetic resonant coupling. The selection of frequency for power transfer is the most crucial part, as the basic restriction (BR) criteria proposed by ICNIRP guidelines and the IEEE C95.1 standard need to be followed, which ensures the safety of the patient. This is suggested by considering some basic restriction parameters, such as specific absorption rate (SAR) and current density, as suggested by guidelines. In this paper, experimentation using two frequencies is shown, i.e., 1.47 MHz (the high frequency) and 62 KHz (the low frequency). For experimentation, goat flesh and saline solution are used. Secondary coil and flesh are dipped in the saline solution. Battery recharging performed at a lower frequency took less time than with a frequency in the MHz range. All BR criteria are fulfilled for both frequencies, so the proposed methodology is safe to use.

KEYWORDS

wireless power transfer (WPT), active implantable medical devices (AIMDs), basic restrictions (BR)

1 INTRODUCTION

With the day-to-day rise in cardiovascular diseases such as problems of arrhythmia (bradycardia or tachycardia), i.e., irregular heartbeats, active implantable medical devices (AIMDs) such as implantable cardioverter defibrillators (ICDs) and pacemakers are the only solution and are in large demand nowadays. Similarly,

Newaskar, D., Patil, B.P. (2023). Rechargeable Active Implantable Medical Devices (AIMDs). *International Journal of Online and Biomedical Engineering (iJOE)*, 19(13), pp. 108–119. <https://doi.org/10.3991/ijoe.v19i13.41197>

Article submitted 2023-05-07. Revision uploaded 2023-07-05. Final acceptance 2023-07-11.

© 2023 by the authors of this article. Published under CC-BY.

AIMDs such as cochlear implants or intracranial pressure (ICP) monitoring devices, which are mostly used in emergency brain injury cases to monitor the pressure inside the cerebrospinal fluid and the brain tissue, are in great need. Along with data logging operations, AIMDs deliver electrical signals to some organs or tissues [1–8]. As these devices are implanted inside the patient's body, the only source of power is the battery. Generally, lithium-ion batteries are used to supply these devices, as they have a longer shelf life and a very slow discharge rate. The battery occupies almost half of the device's size. To have a longer life, demands more energy density of a battery which in turn increases its size. The proposed idea is that if a smaller rechargeable battery is used, then with wireless power transfer charging technology, the implantable device size can be reduced, and at the same time, the life of the device can be increased. The design of the coils used for wireless power transfer is a crucial task because of the size constraint on the secondary coil, which will be placed on the implanted device inside the human body [9–16].

2 SOME BASIC RESTRICTIONS

Guidelines as specified by the IEEE C95.1 standard and ICNIRP must be followed while charging the battery in wireless mode. These standards provide certain basic restrictions (BR) imposed on certain parameters, such as specific absorption rate (SAR), current density, and power density, for operations in different frequency ranges. Neglecting these restrictions can cause a rise in body temperature due to heating. As per human physiology, a rise in the temperature of a human body exceeding a certain value causes a breakdown of the nervous system and protein insolubility. If the temperature of the body rises to 41°C, a person may suffer a seizure. Beyond 43°C of body temperature, a human being cannot even survive. Table 1 shows threshold current ranges and their effects at different frequencies. Table 2 indicates maximum contact current values for different frequencies that will not cause any harm to the human body [17–20].

Table 1. Threshold current ranges and their effect for different frequencies [18]

Indirect Effect	Threshold Current (mA) at Frequency		
	50/60 Hz	1 kHz	100 KHz
Touch perception	0.2 to 0.4	0.4 to 0.8	25 to 40
finger contact pain	0.9 to 1.8	1.6 to 3.3	33 to 55
painful shock threshold	8 to 16	12 to 24	112 to 224
Heavy shock or difficulty in breathing	12 to 23	21 to 41	160 to 320

Table 2. Maximum contact current values for different frequencies which is not harmful [18]

Exposure Type	Range of Frequency	Maximum Contact Current (mA)
Service exposure	Up to 2.5KHz	1
	2.5 to 100 KHz	0.4*f
	100 KHz to 10 MHz	40
General people exposure	Up to 2.5 KHz	0.5
	2.5 to 100 KHz	0.2*f
	100 KHz to 10 MHz	20

Maximum contact current defines the maximum allowed level for contact current generated in the body for different frequency ranges, which will not cause damage to the tissues and won't show biological effects due to contact currents such as shock or burn hazards. If the human body gets in contact with an object at a different potential, contact currents are generated, especially when the potential is induced by an electromagnetic field.

3 SELECTION OF RANGE OF FREQUENCIES FOR WPT

Two inductively coupled coils with wireless power transfer technology are illustrated in Figure 1. Operational frequency selection for transferring power wirelessly is the most critical aspect, as the transferred power should not damage the tissues of the patient wearing the device.

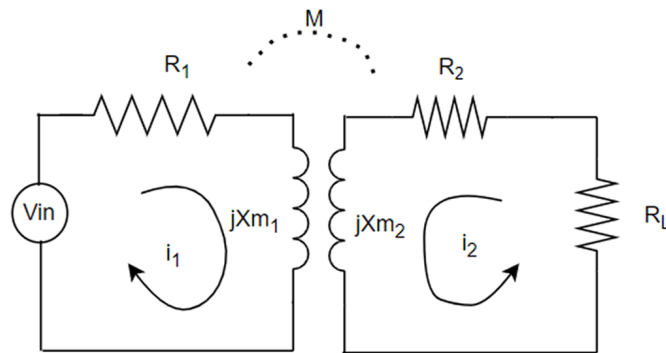


Fig. 1. Circuit for inductively coupled coils

Applying Kirchhoff's current law to the primary and secondary sides, we get

$$R_1 i_1 + jX_{m1} i_2 = V_{in} \quad (1)$$

$$R_2 i_2 + R_L i_2 - jX_{m2} i_1 = 0 \quad (2)$$

Solving further,

Where R_1 is the internal resistance of the primary coil and R_2 is the internal resistance of the secondary coil. i_1 is the current flowing through the primary loop, whereas i_2 is the current flowing through the secondary loop. X_{m1} and X_{m2} are the impedances offered by the primary and secondary inductances, respectively.

$$\eta = \frac{R_L}{(R_2 + R_L) \left\{ 1 + \frac{R_1 (R_2 + R_L)}{\omega^2 M^2} \right\}} \quad (3)$$

Here η denotes the efficiency of power transfer.

The magnetic field produced by lower frequencies will penetrate deeply into the body, and at the same time, the efficiency of power transfer will be compromised. Higher frequencies will have more transfer efficiency, as shown in (3), but they will cause eddy current losses, which in turn cause heating of tissues and may cause electromagnetic interference in the working of AIMD. So, selecting the optimum frequency for transferring power is a critical issue. It must be as high as possible to have more efficiency, but at the same time, it should adhere to the guidelines

provided by ICNIRP. So, the minimum and maximum frequency ranges are calculated considering basic restrictions. The guidelines provided by ICNIRP are more stringent than those specified by IEEE C95.1 [17–20]. These restrictions are provided on time-varying electric, magnetic, and electromagnetic fields, considering some established health effects. Depending on the frequency used for power transfer, restrictions are specified on some physical quantities such as current density (J), specific energy absorption rate (SAR), and power density (S).

As per ICNIRP guidelines as well as the IEEE C 95.1 standard, for frequencies ranging from 1 KHz to 100 KHz, only the current density parameter needs to be considered as a basic restriction, whereas for frequencies ranging from 100 KHz to 10 MHz, the current density as well as the SAR need to be considered as basic restrictions.

3.1 Mathematical calculations to select the operating frequency for wireless power transfer

Considering basic restrictions such as SAR, it can be mathematically specified as:

$$\text{SAR} = \frac{\sigma(|E|^2)}{\rho} \text{ W/Kg} \quad (4)$$

σ is the conductivity of tissue [conductivity of heart muscle ≈ 2.69 S/m].

ρ is the mass density of tissue in Kg/m³

E is the rms electric field V/m.

Considering the mass density of tissues such as blood, fat, and skin, the frequency range for power transfer is calculated as follows.

Case I: Considering the mass density of tissue of fat and breast fat as $\rho = 911$ kg/m³ as specified in the SWISS IT'IS database, which states biological tissues dielectric property. Considering the maximum allowed SAR value as 2W/Kg (localized SAR limit for general public-head and trunk area), referring to equation 4,

$$2 = \frac{2.69 \times (|E|^2)}{911}$$

$$\therefore E = 26.02 \text{ V/m}$$

So, electric field intensity needs to be within 26.02 V/m.

As per Ohm's law,

$$J = \sigma \times E \text{ A/m}^2 \quad (5)$$

$$J = 2.69 \times 26.02$$

$$= 70 \text{ A/m}^2$$

Therefore, current density J needs to be within 70 A/m².

As per ICNIRP guidelines, exposure limits for current density parameters for frequencies in the range of 100 KHz to 10 MHz must be less than $f/500$ mA/m².

$$J \leq \frac{f}{500} \quad (6)$$

So, substituting the values in the equation, the frequency used for power transfer must be less than 35MHz.

Case II: Considering the mass density of tissue of skin as $\rho = 1109 \text{ kg/m}^3$,

$$E = 28.714 \text{ V/m}$$

$$\therefore J \leq 77.24 \text{ A/m}^2$$

So, the frequency used for power transfer must be less than 38.6 MHz.

Case III: Considering the mass density of tissue of the lungs as $\rho = 394 \text{ kg/m}^3$,

$$E = 17.11 \text{ V/m}$$

$$\therefore J = 46.03 \text{ A/m}^2$$

So, the frequency used for power transfer must be less than 23 MHz.

Thus, from the above three cases, the optimum frequency for the power transfer can be concluded to be less than 23 MHz.

Different coils with different numbers of turns were designed for experimentation and tested for different frequencies for power transfer. A lithium-ion battery must be charged with a constant voltage supply. It is provided by the rectifier circuit connected on the secondary side. To fulfill this requirement, the supply voltage from the signal generator was set to approximately 20 Volts peak to peak. But for a higher frequency range for power transfer, the supply current from the function generator is lower, resulting in a lower output current. Though a constant voltage was applied to the battery to recharge it, the charging current was lower, resulting in more time required to charge the battery. To have current in the mA range, the higher frequency for power transfer is considered 1.5 MHz, for which the current density and specific absorption rate are considered basic restriction (BR) parameters by ICNIRP. For frequencies below 100 KHz, current density is the only BR that needs to be considered. So, another frequency for power transfer is considered to be 62 KHz, i.e., less than 100 KHz.

4 HIGH-FREQUENCY RECTIFIER CIRCUIT AND WPT DESIGN

The WPT setup is designed for 1.5 MHz. The high-frequency rectifier circuit is designed using N-MOSFETS, as a normal rectifier circuit using diodes fails to function for the high-frequency range in MHz. Figure 2 shows a high-frequency rectifier circuit designed in multisim. The circuit is designed using N-channel enhancement-mode MOSFETs.

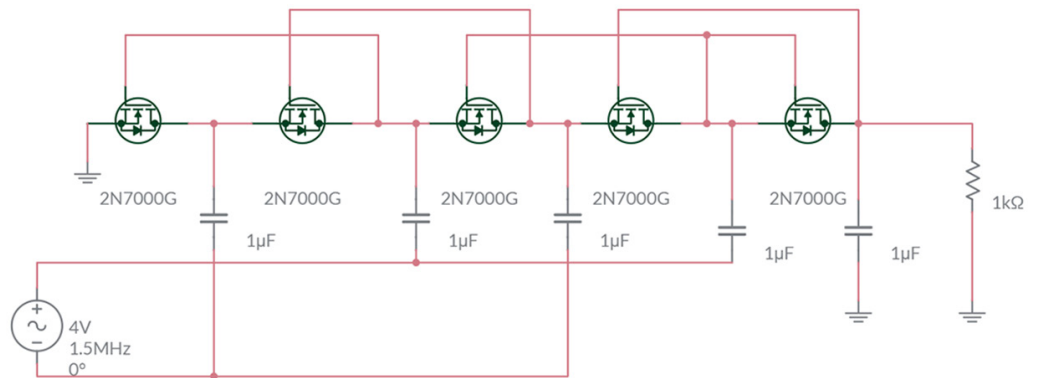


Fig. 2. High-frequency rectifier circuit

5 SPECIFICATIONS AND DESIGN OF WPT

The basic idea for WPT, showing two coils coupled inductively with a separation distance d selected at a minimum of 0.8 cm, is shown in Figure 3. The distance between two coils is chosen considering the thickness of the skin, fat, and muscles. Primary side coil L_p is considered to be outside the patient’s body, while secondary side coil L_s is considered to be inside the body while wearing AIMD. The L_p coil is supplied with an input signal with the desired frequency. Emf will be induced in the secondary coil by the electromagnetic induction principle.

The compensation capacitor value is selected to have maximum power transfer at a particular frequency. The primary coil L_p is parallelly compensated as the capacitance compensates the primary coil current. So, the input current requirement from the supply is reduced. Secondary coil L_s is series compensated as the capacitance-voltage compensating the voltage across the primary reactance, causing the output voltage to be independent of the load resistance [21–28].

The compensation capacitor value is designed using the relation,

$$f_r = \frac{1}{2\pi\sqrt{LC}} \tag{7}$$

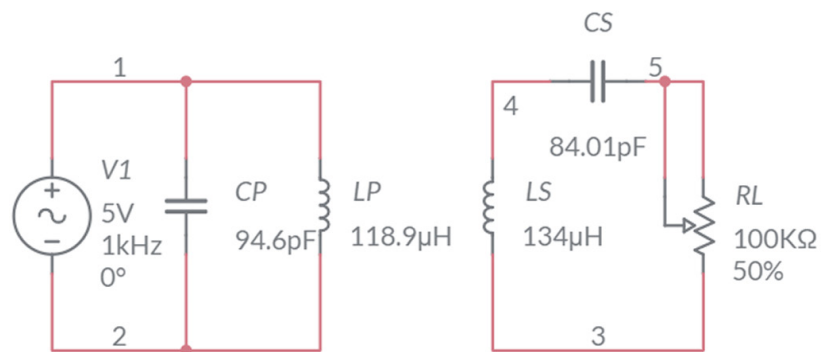


Fig. 3. Coil set up used with specifications

Table 3. Specifications of coils used in the set up for frequency 1.47 MHz

Parameters	Primary Coil	Secondary Coil
Inductance	$L_p = 118.9 \mu\text{H}$	$L_s = 134 \mu\text{H}$
Turns	41	41
Q	0.3031	0.3334
R_s	2.462Ω	2.529Ω
Radius	2 cm	2 cm

Gauge of coil used = 38. i.e., $d = 1.007 \text{ mm}$
 $r = 0.05035 \text{ mm}$
 $V_{in} = 20 \text{ Vpp}$ for frequency 1.47 MHz
 $C_p = 94.6 \text{ pF} \approx 97.99 \text{ pF}$
 $C_s = 84.014 \text{ pF} \approx 70.31 \text{ pF}$
 Primary parallel and secondary series compensation
 $R_L = 100 \text{ K}\Omega$ pot
 To measure current: GWINSTEK GDM8261A 6 ½ digit Digital Multimeter is used.

The lithium-ion battery is selected for the experimentation as it has a slow discharge rate, a high shelf life, and a high energy density, which makes it suitable for AIMD purposes [29–33]. Table 3 shows the specifications of the coils used in the setup for a frequency of 1.47 MHz for power transfer.

Figure 4 shows a graph drawn for the percentage of battery charge versus the time required for charging the 3.7 V lithium-ion 300 mAh battery. The frequency used for WPT is 1.47 MHz and secondary current, 1 mA approximately.

Generally, a lithium-ion battery will be topped up as soon as it discharges up to 85 percent of its full charge. So, with a shallow discharge, it will be topped off with a full charge. From Figure 4, it can be noted that the time required to charge from 85% to 100% is approximately 180 minutes, i.e., up to 3 hours. The charging process took too long to recharge since the charging current is too low since the supply current by the function generator is limited for higher frequencies for maximum input voltage because of bandwidth constraints. The input voltage was set to maximum, i.e., 20 Vpp. Since we need to charge a lithium-ion battery, we need constant voltage at the output. i.e., at least 4 V to 4.2 V, the output of the rectifier after passing through an air medium and flesh in between. So the maximum input voltage needs to be delivered.

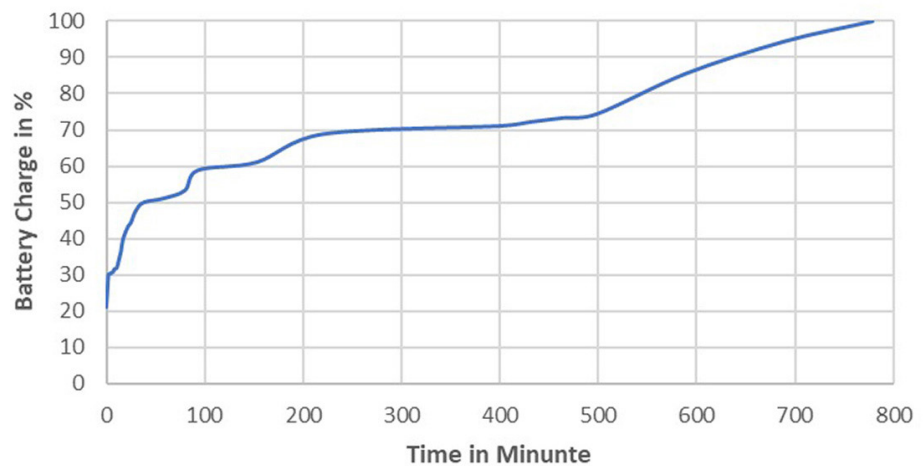


Fig. 4. Plot of percentage charging of a battery with respect to time for 1.47 MHz frequency

6 LOWER FREQUENCY USED FOR WPT

Specifications of coils used for WPT using freq. 62 kHz are as shown below in Table 4.

Table 4. Specifications of coils used for WPT using frequency 62 KHz

Parameters	Primary Coil	Secondary Coil
Inductance	L1 = 3.5 mH	L2 = 1.733 mH
Turns	250	200
Radius	3.5 cm	1.5 cm

Gauge of coil used = 38. i.e., $d = 1.007$ mm, $r = 0.05035$ mm
 $V_{in} = 20$ Vpp for frequency 62 kHz
 Primary parallel and secondary series compensation
 To measure current: GWINSTEK GDM8261A 6 ½ digit Digital Multimeter is used.

For frequencies below 100 KHz, the basic restriction is imposed only on the current density parameter. So, the frequency for power transfer is chosen to be less than 100 kHz, i.e., 62 KHz. The coils were designed with the design restrictions in mind. As the secondary coil will be mounted on the pacemaker, it has size restrictions. But there is no restriction on the size of the primary coil. It is kept large to compensate for any misalignment of the two coils.

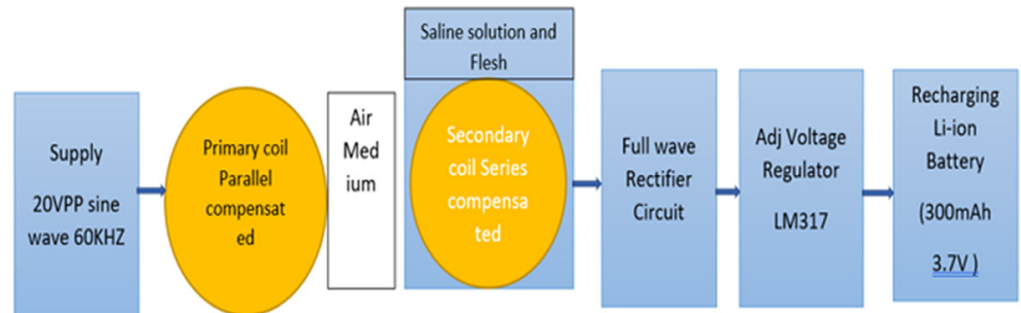


Fig. 5. Block diagram representation of the actual set up used to charge the battery

Figure 5 depicts the block diagram of the actual setup used to charge the battery. Readings are taken with the two coils separated 0.8 cm (skin layer, tissues, and muscle layer) apart with an air medium in between. Readings are noted when both coils are in the air. A full-wave rectifier circuit is designed using 1N4148 switching diodes followed by an adjustable voltage regulator, LM317. The output of the regulator circuit is used to charge the battery. Then the secondary coil is kept inside the saline solution, as shown in Figure 6, and readings are taken. The saline solution is used for experimentation as its characteristics are similar to those of blood. The time taken by the battery to charge is noted. Lastly, the flesh is kept over the secondary coil dipped inside the saline solution depicted in Figure 7. A saline solution is chosen because it resembles the characteristics of blood.

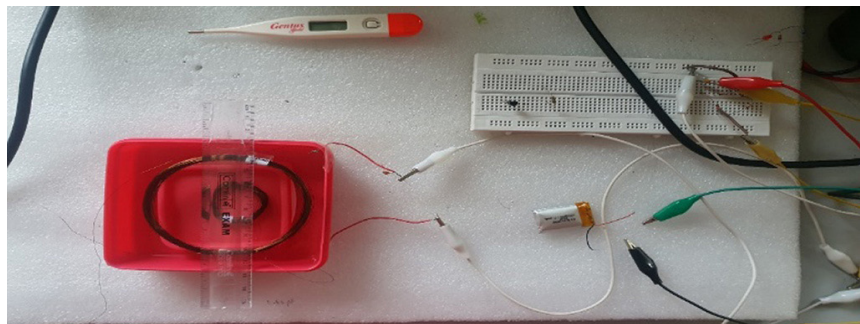


Fig. 6. Experiment setup where secondary coil is placed inside saline solution

As specified in ICNIRP guidelines, for frequency $f < 100$ KHz, current density $J < f/500$ mA/m² for general public exposure.

For frequency, $f = 62$ kHz, the current density must be less than 0.124 A/m². Since the maximum current through the device is 4.23 mA. Average current density over 1 cm² it is less than 0.124 A/m² [34–36].

Since the current at 62 kHz is larger than flowing in the MHz frequency scale, the recharging time at 62 kHz would be shorter.

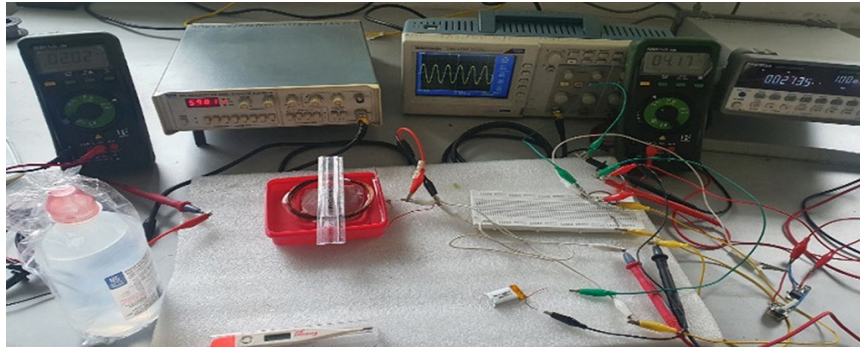


Fig. 7. Experiment set up: secondary coil kept inside saline solution with flesh in between the primary coil and secondary coil

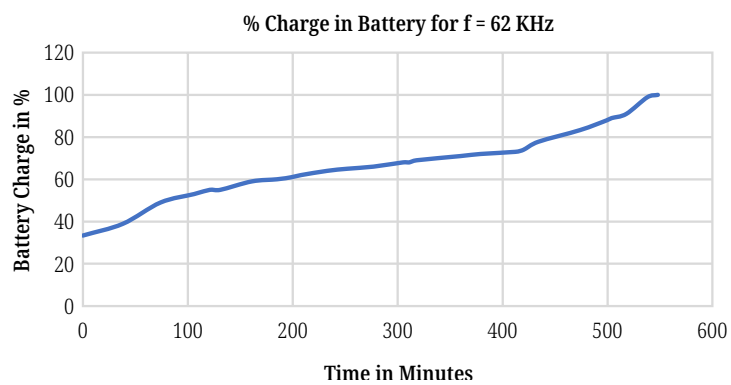


Fig. 8. Plot of percentage charging of a battery with respect to time for 62 kHz frequency

As specified in Table 2, for frequencies in the range of 2.5 to 100 kHz, the current should be less than or equal to $0.2 \cdot f$ mA where f is in kHz.

$$\text{Current} \leq 0.2 \cdot 60 \text{ mA} = 12 \text{ mA.}$$

Since the maximum current flowing through the secondary winding is not exceeding this level, there won't be any painful shocks or hazardous conditions.

Figure 8 depicts that the time required to charge the battery from 85% to full charge is approximately 90 minutes, i.e., 1 hour and 30 minutes, approximately causing no tissue heating or any adverse effect since the BR parameters are within the range as specified by guidelines.

7 CONCLUSIONS

From the results, it is evident that the current through the device is within the range specified by the guidelines. The patient would not feel touch perception or pain at the fingertip, let-go or painful shock, or any difficulty in breathing.

The recharging experiments were successfully performed, satisfying all the criteria specified by the ICNIRP guidelines and following the IEEE C95.1 standard. This ensures the safety of patients undergoing recharging. A patient would not suffer from tissue damage as well as damage to the central nervous system.

For both power transfer using a high frequency, i.e., 1.47 MHz, as well as a lower frequency, i.e., 62 kHz, the basic restrictions are satisfied. Less time is required for the battery to charge with WPT at 62 kHz. It took almost 90 minutes, i.e., 1 hour and 30 minutes, to charge from 85% of its residual capacity to 100%.

The current produced in the secondary coil does not exceed the maximum contact current (mA) as specified by ICNIRP guidelines for both cases. So, the proposed methodology is novel and safe to implement as long as all BR criteria are fulfilled.

8 REFERENCES

- [1] T. Campi, S. Cruciani, V. De Santis, F. Palandrani, A. Hirata, and M. Feliziani, "Wireless Power Transfer Charging System for AIMDs and Pacemakers," *IEEE Trans. Microw. Th. Techn.*, vol. 64, no. 2, pp. 633–642, 2016. <https://doi.org/10.1109/TMTT.2015.2511011>
- [2] C. Xiao, K. Wei, D. Cheng, and Y. Liu, "Wireless Charging System Considering Eddy Current in Cardiac Pacemaker Shell: Theoretical Modeling, Experiments, and Safety Simulations," *IEEE Transactions on Industrial Electronics*, vol. 64, no. 5, pp. 3978–3988, 2017. <https://doi.org/10.1109/TIE.2016.2645142>
- [3] L. Chen, S. Liu, Y.C. Zhou, and T.J. Cui, "An Optimizable Circuit Structure for High-Efficiency Wireless Power Transfer," *IEEE Transactions on Industrial Electronics*, vol. 60, no. 1, pp. 339–349, 2013. <https://doi.org/10.1109/TIE.2011.2179275>
- [4] T. Campi, S. Cruciani, G.P. Santilli, and M. Feliziani, "Numerical analysis of EMF safety and thermal aspects in a pacemaker with a Wireless Power Transfer System," *IEEE Wireless Power Transfer Conference (WPTC)*, Boulder, CO, USA, pp. 1–4, 2015. <https://doi.org/10.1109/WPT.2015.7140172>
- [5] T. Campi, S. Cruciani, M. Feliziani, and A. Hirata, "Wireless power transfer system applied to an active implantable medical device," *IEEE Wireless Power Transfer Conference*, Jeju, Korea (South), pp. 134–137, 2014. <https://doi.org/10.1109/WPT.2014.6839612>
- [6] T. Campi, S. Cruciani, V. De Santis, F. Palandrani, F. Maradei, and M. Feliziani, "Induced Effects in a Pacemaker Equipped with a Wireless Power Transfer Charging System," *IEEE Transactions on Magnetics*, vol. 53, no. 6, pp. 1–4, 2017. <https://doi.org/10.1109/TMAG.2017.2661859>
- [7] X. Zhang, S.L. Ho, and W.N. Fu, "A Hybrid Optimal Design Strategy of Wireless Magnetic-Resonant Charger for Deep Brain Stimulation Devices," *IEEE Transactions on Magnetics*, vol. 49, no. 5, pp. 2145–2148, 2013. <https://doi.org/10.1109/TMAG.2013.2244585>
- [8] Y. Yu, H. Hao, W. Wang, and L. Li, "Simulative and experimental research on wireless power transmission technique in implantable medical device," Annual International Conference of the *IEEE Engineering in Medicine and Biology Society*, Minneapolis, MN, USA, pp. 923–926, 2009. <https://doi.org/10.1109/IEMBS.2009.5332831>
- [9] U.M. Jow and M. Ghovanloo, "Design and Optimization of Printed Spiral Coils for Efficient Inductive Power Transmission," 14th *IEEE International Conference on Electronics, Circuits and Systems*, Marrakech, Morocco, pp. 70–73, 2007. <https://doi.org/10.1109/ICECS.2007.4510933>
- [10] U.M. Jow and M. Ghovanloo, "Modeling and Optimization of Printed Spiral Coils in Air, Saline, and Muscle Tissue Environments," *Transactions on Biomedical Circuits and Systems*, vol. 3, no. 5, pp. 339–347, 2009. <https://doi.org/10.1109/TBCAS.2009.2025366>
- [11] I.M. Khan, S. Khan, and O.O. Khalifa, "Wireless Transfer of Power to Low Power Implanted Biomedical Devices: Coil Design Considerations," *IEEE International Instrumentation and Measurement Technology Conference Proceedings*, Graz, Austria, pp. 1–5, 2012. <https://doi.org/10.1109/I2MTC.2012.6269384>
- [12] L.R. Clare, S.G. Burrow, B.H. Stark, N.J. Grabham, and S.P. Beeby, "Design of an Inductive Power Transfer System with Flexible Coils for Body-worn Applications," *J. Phys.: Conf. Ser.* 660 012135, vol. 660, 2015. <https://doi.org/10.1088/1742-6596/660/1/012135>

- [13] A. Ben, A.B. Kouki, and H. Cao, "Power Approaches for Implantable Medical Devices," *Sensors (Basel)*, vol. 15, no. 11, pp. 28889–28914, 2015. PMID: 26580626; PMCID: PMC4701313. <https://doi.org/10.3390/s151128889>
- [14] Q.S. Ahmad, T.A. Chandel, and S. Ahmad, "Wireless Power Transmission to Charge Pacemaker Battery," *Journal of Physics: Conference Ser.* 660 012135, vol. 660, 2015.
- [15] D. Newaskar and B.P. Patil, "Wireless Power Transfer through Inductive Coupling for AIMDs," *International Journal of Innovative Technology and Exploring Engineering (IJITEE)*, vol. 8, no. 11, 2019. <https://doi.org/10.35940/ijitee.K1258.0981119>
- [16] B.P. Patil, D. Newaskar, K. Sharma, T. Baghmar, and M. Rajput, "Effect of Number of Turns and Medium between Coils on the Wireless Power Transfer Efficiency of AIMDs," *Biomedical Engineering Applications Basis and Communications*, vol. 31, no. 02, 2019. <https://doi.org/10.4015/S1016237219500169>
- [17] IEEE Standard for *Safety Levels with Respect to Human Exposure to Electric, Magnetic, and Electromagnetic Fields*, 0 Hz to 300 GHz, IEEE Std C95.1™-2019.
- [18] Int. Commission Non-Ionizing Radiat. Protection, "Guidelines for Limiting Exposure to Time-Varying Electric, Magnetic, and Electromagnetic Fields (up to 300 GHz)," *Health Phys.*, vol. 74, pp. 494–522, 1998.
- [19] IEEE Standard for *Safety Levels with Respect to Human Exposure to Radio Frequency Electromagnetic Fields*, 3 kHz to 300 GHz, IEEE Standard C95.1, 2005.
- [20] Int. Commission Non-Ionizing Radiat. Protection, "Guidelines for Limiting Exposure to Time-Varying Electric and Magnetic Fields for Low Frequencies (1 Hz–100 kHz)," *Health Phys.*, vol. 99, pp. 818–836, 2010. <https://doi.org/10.1097/HP.0b013e3181f06c86>
- [21] C.S. Wang, G.A. Covic, and O.H. Stielau, "Power Transfer Capability and Bifurcation Phenomena of Loosely Coupled Inductive Power Transfer Systems," *IEEE Trans. Ind. Electron.*, vol. 51, no. 1, pp. 148–157, 2004. <https://doi.org/10.1109/TIE.2003.822038>
- [22] X. Liu, L. Clare, X. Yuan, C. Wang, and J. Liu, "A Design Method for Making an LCC Compensation Two-Coil Wireless Power Transfer System More Energy Efficient than an SS Counterpart," *Energies*, vol. 10, no. 9, p. 1346, 2017. <https://doi.org/10.3390/en10091346>
- [23] Y. Liao and X. Yuan, "Compensation Topology for Flat Spiral Coil Inductive Power Transfer Systems," *IET Power Electronics* vol. 8, no. 10, 2015. <https://doi.org/10.1049/iet-pel.2014.0589>
- [24] R. Porto, L. Murliky, G. Oliveira, and V. Brusamarello, "Multivariable Automatic Compensation Method for Inductive Power Transfer System," vol. 1, pp. 1–6, 2017. <https://doi.org/10.1109/EEEIC.2017.7977659>
- [25] A.P. Sample, D.T. Meyer and J.R. Smith, "Analysis, Experimental Results, and Range Adaptation of Magnetically Coupled Resonators for Wireless Power Transfer," *IEEE Transactions on Industrial Electronics*, vol. 58, no. 2, pp. 544–554, 2011. <https://doi.org/10.1109/TIE.2010.2046002>
- [26] V.S. Mallela, V. Ilankumar, and N. Srinivasa Rao, "Trends in Cardiac Pacemaker Batteries," *Indian Pacing and Electrophysiology Journal*, vol. 4, pp. 201–212, 2004.
- [27] E. Gati, S. Kokosis, N. Patsourakis, and S. Manias, "Comparison of Series Compensation Topologies for Inductive Chargers of Biomedical Implantable Devices," *Electronics*, vol. 9, no. 1, p. 8, 2020. <https://doi.org/10.3390/electronics9010008>
- [28] C. Liu and G. Shi, "Automatic Compensation Device for Distribution Line Based on Wireless Sensor," *International Journal of Online and Biomedical Engineering (ijOE)*, vol. 13, no. 05, pp. 160–173, 2017. <https://doi.org/10.3991/ijoe.v13i05.7058>
- [29] D. Newaskar and B.P. Patil, "Wireless Charging of AIMDs-Compensation Circuits," *International Conference on Computational Performance Evaluation (ComPE)*, Shillong, India, pp. 173–177, 2020. <https://doi.org/10.1109/ComPE49325.2020.9200101>

- [30] M. Harry and F. Gary, "The Cardiac Implantable Electronic Device Power Source: Evolution and Revolution," *Pacing and Clinical Electrophysiology (PACE)*, vol. 37, no. 12, pp. 1728–1745, 2014. <https://doi.org/10.1111/pace.12526>
- [31] F. Untereker, L. Darrel, Craig. Schmidt, Gaurav Jain, A. Prabhakar, Tamirisa, Joachim Hossick-Schott, and Mark Viste, "8 – Power Sources and Capacitors for Pacemakers and Implantable Cardioverter-Defibrillators," pp. 251–269, 2017. <https://doi.org/10.1016/B978-0-323-37804-8.00008-0>
- [32] D. Newaskar and B.P. Patil, "Batteries for Active Implantable Medical Devices," *International Conference on Intelligent Technologies (CONIT), IEEE*, pp. 1–7, 2021. <https://doi.org/10.1109/CONIT51480.2021.9498319>
- [33] Z. Haizhou, "Modeling of Lithium-Ion Battery for Charging/Discharging Characteristics Based on Circuit Model," *International Journal of Online and Biomedical Engineering (iJOE)*, vol. 13, no. 06, pp. 86–95, 2017. <https://doi.org/10.3991/ijoe.v13i06.6799>
- [34] IT²S foundation, "Tissue Properties," <https://itis.swiss/virtual-population/tissue-properties/database>
- [35] H.P. Schwan and C.F. Kay, "Specific Resistance of Body Tissues," vol. 4, no. 6, pp. 664–670, 1956. <https://doi.org/10.1161/01.RES.4.6.664>
- [36] K. Djennah, A. Ladjimi, and A. Babouri, "In Vitro Modeling of Implantable Cardiac Pacemakers Submitted to Conducted Disturbance," *International Journal of Online and Biomedical Engineering (iJOE)*, vol. 18, no. 01, pp. 65–77, 2022. <https://doi.org/10.3991/ijoe.v18i01.27289>

9 AUTHORS

Mrs. Deepali Newaskar is a life member of ISTE. She is currently working as an Assistant Professor in the Department of Electronics and Telecommunication Engineering in RMD Sinhgad Technical Institute Campus, Pune and also is a Research Scholar at Sinhgad College of Engineering, Savitribai Phule Pune University, Pune, India. She has 14 years of teaching experience and has published 14 papers both at national and international conferences and journals. Her research interest include wireless power transfer, biomedical engineering, Machine Learning, and Signal Processing.

B. P. Patil is currently working as Principal of Army institute of Technology, Pune. He is having 28 years of teaching and 5 years of industry. He has received the "Sir Thomas Ward Memorial Medal" from the Institution of Engg., Calcutta, for the best paper in E & T Journal div. for the year 1999–2000. He was felicitated with "Education Leadership Award" by Dewang Mehta and is ranked in "50 Most Influential Principals of India." He has published 172 papers both at national and international conferences and journals. He has Published 02 books, filed 07 patents, and 5 copyrights. He is Sr. Member of IEEE, Fellow of IETE, Institution of Engineers and Life member of ISTE and Instrument Society of India. His research interest includes wireless communication, biomedical signal processing and non-conventional energy.